Envirosoft 86

Proceedings of the International Conference on Development and Application of Computer Techniques to Environmental Studies, Los Angeles, U.S.A., November 1986

Editor:
P. Zannetti

Computational Mechanics Publications

The Choice of Which Hydrologic Model to Use

T.V. Hromadka II
Director, Water Resources Division, Williamson and Schmid, Irvine, CA, and Research Associate, Princeton University, NJ, U.S.A.
A.J. Nestlinger
Hydrologist, Orange County Environmental Management Agency, Santa Ana, CA, and Administrative Director, Computational Hydrology International, Santa Ana, U.S.A.

ABSTRACT

For Southern California watersheds, as is the case for most watersheds in the United States, rainfall-runoff data are relatively sparse such that the calibration of a hydrologic model is uncertain. With the large number and types of hydrologic models currently available, the choice of the "best" hydrologic model to use is not clear. Because of the limited data, the hydrologic model must be simple in order to validate parameter values and submodel algorithms. Due to the uncertainty in stream gauge data frequency analysis, a level of confidence (e.g. 85%) should be chosen to provide a level of protection against a specified flood return frequency (e.g. 100-year). Due to the calibrated model range and distribution of possible outcomes caused by uncertainty in modeling parameter values, the use of a regionally calibrated model at an ungauged catchment needs to address the probability that the hydrologic model estimate of flood quatities (e.g. peak flow rates) achieves the level of protection for a specified flood level. In this paper, a design storm unit hydrograph model is developed and calibrated with respect to model parameter values and with respect to runoff frequency tendencies (design storm) in order to address each of these issues.

INTRODUCTION

Fundamental to the preparation of a policy statement for the development of flood control system design values are the decisions of (1) the specific hydrologic model to adopt; (2) the selection of calibration data sets; (3) the selection of a desired level of flood protection (e.g., 100-year flood, or other); and (4) the selection of a level of certainty in achieving the level of flood protection. Each of these decision points, must be considered in formulating a policy. This paper provides a discussion of each of the points and the factors that were considered in formulating a flood control and drainage policy for a county in southern California.

RUNOFF HYDROGRAPH MODEL PARAMETERS

The design storm unit hydrograph model ("model") is based upon several parameters; namely, two loss rate parameters (a phi index coupled with a fixed percentage), an S-graph, catchment lag, storm pattern (shape, location of peak rainfalls, duration), depth-area (or depth-area-duration) adjustment, and the return frequency of rainfall.

Loss Function

The loss function, f(t), used in the "model" is defined by

$$f(t) = \begin{cases} \bar{Y}I(t), \text{ for } \bar{Y}I(t) < Fm \\ Fm, \quad \text{otherwise} \end{cases} \tag{1}$$

where $\bar{Y}$ is the low loss fraction and Fm is a maximum loss rate defined by

$$Fm = \sum ap_j \; Fp_j \tag{2}$$

where ap_j is the actual pervious area fraction with a corresponding maximum loss rate of Fp_j; the infiltration rate for impervious area is set at zero; and I(t) is the design storm rainfall intensity at storm time t.

The use of a constant percentage loss rate $\bar{Y}$ in Eq. 1 is reported in Scully and Bender (1969), Williams et al. (1980), and Schilling and Fuchs (1986). The use of a phi index (ϕ - index) method in effective rainfall calculations is also well-known (e.g., Kibler, 1982).

The low loss rate fraction is estimated from the SCS loss rate equation (U.S. Dept. of Agric., 1972) by

$$\bar{Y} = 1-Y \tag{3}$$

where Y is the catchment yield computed by

$$Y = \sum a_j \; Y_j \tag{4}$$

In Eq. 4, Y_j is the yield corresponding to the catchment area fraction a_j and is estimated using the SCS curve number (CN) by

$$Y_j = \frac{(P_{24} - Ia)^2}{(P_{24} - Ia + S)\,P_{24}} \tag{5}$$

where P_{24} = the 24-hour T-year precipitation depth; Ia is the initial abstraction of Ia = 0.2S; and S = (1000/CN)-10.

From the above relationships, the low loss fraction, $\bar{Y}$, acts as a fixed loss rate percentage, whereas Fm serves as an upper bound to the possible values of $f(t) = \bar{Y}I(t)$.

Values for Fm are based on the actual pervious area cover percentage (a_p) and a maximum loss rate for the pervious area, F_p. Values for F_p are developed from rainfall-runoff calibration studies of several significant storm events for several watersheds within the region under study. Further discussions regarding the estimation of parameter values are contained in a subsequent section.

A distinct advantage afforded by the loss function of Eq. 1 over loss functions such as Green-Ampt or Horton is that the effect of the location of the peak rainfall intensities in the design storm pattern on the model peak flow rate (Q) becomes negligible. That is, front-loaded, middle-loaded, and rear-loaded storm patterns all result in nearly equal peak flow estimates. Consequently, the shape (but not magnitude) of the design storm pattern is essentially eliminated from the list of parameters to be calibrated in the runoff hydrograph "model" (although the time distribution of runoff volumes are affected by the location of the peak rainfalls in the storm pattern which is a consideration in detention basin design).

S-Graph

The S-graph representation of the unit hydrograph (e.g., McCuen and Bondelid (1983), Chow and Kulandalswamy (1982), Mays and Coles (1980)) can be used to develop unit hydrographs corresponding to various watershed lag estimates. The S-graph was developed by rainfall-runoff calibration studies of several storms for several watersheds. By averaging the S-graphs for each watershed studied, a representative

S-graph is developed for each watershed. By comparing the representative S-graphs, regional S-graphs were derived to represent the average of watershed-averaged S-graphs.

Lag

Fundamental to any hydrologic model is a catchment timing parameter. For the "model", watershed lag is defined as the time from the beginning of effective rainfall to that time corresponding to 50-percent of the S-graph ultimate discharge. To estimate catchment lag, it is assumed that lag is related to the catchment time of concentration (Tc) as calculated by a sum of normal depth flow calculated travel times; i.e., a mixed velocity method (e.g. Beard and Chang (1979), McCuen, et al. (1984)). To correlate lag to Tc estimates, lag values measured from watershed calibrated S-graphs were plotted against Tc estimates. A least-squares best fit line gives the estimator

$$\text{lag} = 0.80\,Tc \tag{6}$$

Design Storm Pattern

A 24-hour duration design storm composed of nested 5-minute unit intervals (with each principal duration nested within the next longer duration) was adopted as part of the policy. The storm pattern provides equal return frequency rainfalls for any storm duration; i.e., the peak 5-minute, 30-minute, 1-hour, 3-hour, 6-hour, 12-hour, and 24-hour duration rainfalls are all of the selected T-year return frequency. Such a storm pattern construction is found in HEC Training Document No. 15 (1982) which uses a nested central-loaded design storm pattern.

Runoff Hydrograph Model

The "model" produces a time distribution of runoff Q(t) given by the standard convolution integral representation of

$$Q(t) = \int_0^t e(s)\, u(t-s)\, ds \tag{7}$$

where Q(t) is the catchment flow rate at the point of concentration;

$e(s)$ is the effective rainfall intensity; and $u(x)$ is the unit hydrograph developed from the particular S-graph. In Eq. 7, $e(s)$ represents the time distribution of the 24-hour duration design storm pattern modified according to depth-area effects and then further modified according to the loss function definition of Eq. 1.

In the use of Eq. 7 for a particular watershed, an estimate of catchment lag is used to construct a unit hydrograph $u(x)$. Then, based on the catchment area (depth-area adjustment) and loss rate characteristics, $e(s)$ is determined. Because the peak flow rate $Q_p = \max Q(t)$ shows a negligible variation due to a change in storm pattern shape (except for a severe front loaded, near-monotonically decreasing pattern or a rear loaded, near-monotonically increasing pattern); the model parameters that affect Q_p are loss rates ($\bar{Y}$ and F_p), S graphs, lag estimates, depth-area adjustment curve set, and design storm rainfall return frequency. Note that Fm is not a calibration parameter as $Fm = a_p F_p$ where a_p is the actual measured pervious area fraction.

PARAMETER CALIBRATION

Considerable rainfall-runoff calibration data has been prepared by the Corps of Engineers COE for use in their flood control design and planning studies. Much of this information has been prepared during the course of routine flood control studies in Orange County and Los Angeles County, but additional information has been compiled in preliminary form for ongoing COE studies for the massive Santa Ana River project (Los Angeles County Drainage Area, or LACDA). The watershed information available includes rainfall-runoff calibration results for three or more significant storms for each watershed, developing optimized estimates for the S-graph, lag, and loss rate at the peak rainfall intensities. Although the COE used a more rational Horton type loss function which decreases with time, only the loss rate that occurred during the peak storm rainfalls was used in the calibration effort reported herein.

A total of 12 watersheds were considered in detail for our study. Seven of the watersheds are located in Los Angeles County while the other five catchments are in Orange County (Fig. 1). Several other local watersheds were also considered in light of previous COE studies that resulted in additional estimates of loss rates, S-graphs, and lag values. Table 1 provides an itemization of data obtained from the COE studies, and watershed data assumed for catchments considered hydrologically similar to the COE study catchments.

TABLE 1. WATERSHED CHARACTERISTICS

	Watershed Geometry						Calibration Results			
Watershed Name	Area (mi^2)	Length (mi)	Length of Centroid (mi)	Slope (ft/mi)	Percent Impervious (%)	Tc (Hrs)	Storm Date	Peak F_p (inch/hr)	Lag (hrs)	Basin factor
Alhambra Wash[1]	13.67	8.62	4.17	82.4	45	0.89	Feb.78 Mar.78 Feb.80	0.59,0.24 0.35,0.29 0.24	0.62	0.015
Compton2[1]	24.66	12.69	6.63	13.8	55	2.22	Feb.78 Mar.78 Feb.80	0.36 0.29 0.44	0.94	0.015
Verdugo Wash[1]	26.8	10.98	5.49	316.9	20	--	Feb.78	0.65	0.64	0.016
Limekiln[1]	10.3	7.77	3.41	295.7	25	--	Feb.78 Feb.80	0.27 0.27	0.73	0.026
San Jose[2]	83.4	23.00	8.5	60.0	18		Feb.78 Feb.80	0.20 0.39	1.66	0.020
Sepulveda[2]	152.0	19.0	9.0	143.0	24	--	Feb.78 Mar.78 Feb.80	0.22,0.21 0.32 0.42	1.12	0.017
Eaton Wash[1]	11.02[4] (57%)	8.14	3.41	90.9	40	1.05	---	---	---	0.015[7]
Rubio Wash[1]	12.20[5] (3%)	9.47	5.11	125.7	40	0.68	---	---	---	0.015[7]
Arcadia Wash[1]	7.70[6] (14%)	5.87	3.03	156.7	45	0.60	---	---	---	0.015[8]
Compton1[1]	15.08	9.47	3.79	14.3	55	1.92	---	---	---	0.015[8]
Dominguez[1]	37.30	11.36	4.92	7.9	60	2.08	---	---	---	0.015[8]
Santa Ana Delhi[3]	17.6	8.71	4.17	16.0	40	1.73	---	---	---	0.053[9] 0.040[10]
Westminster[3]	6.7	5.65	1.39	13	40		---	---	---	0.079[9] 0.040[10]
El Modena-Irvine[3]	11.9	6.34	2.69	52	40	0.78	---	---	---	0.028[9]
Garden Grove-Wintersberg[1]	20.8	11.74	4.73	10.6	64	1.98	---	---	---	---
San Diego Creek[1]	36.8	14.2	8.52	95.0	20	1.39	---	---	---	---

Notes 1: Watershed Geometry based on review of quadrangle maps and LACFCD strom drain maps.
2: Watershed Geometry based on COE LACDA Study.
3: Watershed Geometry based on COE Reconstitution Study for Santa Ana Delhi and Westminster Channels (June, 1983).
4: Area reduced 57% due to several debris basins and Eaton Wash Dam reservoir, and groundwater recharge ponds.
5: Area reduced 3% due to debris basin.
6: Area reduced 14% due to several debris basins.
7: 0.013 basin factor reported by COE (subarea characteristics, June, 1984).
8: 0.015 basin factor assumed due to similar watershed values of 0.015.
9: Average basin factor computed from reconstitution studies
10: COE recommended basin factor for flood flows.

Catchment Descriptions

The key catchments utilized for the calibration of the "model" design storm are Alhambra, Arcadia, Compton1 (at 120th Street), Compton2 (at Greenleaf), Dominguez, Eaton, and Rubio Washes. Although other watersheds were considered in the study (see Table 1) for the population of the parameter value distributions, the seven key catchments were considered similar to the region where the "model" is intended for use (the valley area of Orange County) and are used to develop flood frequency estimates.

Four of the seven catchments have been fully urbanized for 20 to 30 years, with efficient interior storm drain systems draining into a major concrete channel. Additionally, all of the major storm events have occurred during the gage record of full urbanization; hence, the gage record can be assumed to be essentially homogeneous (nevertheless, adjustments were made in this study to account for the urbanization effects). Storm drain system maps for the entire catchment were obtained from the Los Angeles County Flood Control District.

Arcadia and Rubio Washes were also fully urbanized and drained except for the foothill areas which account for 14% and 3% of the total catchment area, respectively. In both cases, debris dams (five in Arcadia, one in Rubio) intercept the foothill (most upstream area of the catchment) runoff. The sensitivity of the "model" results to including the foothill area without debris dams versus excluding the foothill area entirely are minor. Due to the increased loss rates and overall catchment lag, inclusion or exclusion of the foothill areas result in less than a ±5% variation in runoff estimates from the "model". Hence, the foothill area was excluded from each of the catchment analysis.

Eaton Wash is also fully urbanized and drained except for 57% of the total catchment area which is upstream of the Eaton Wash dam and water conservation spreading grounds. A review of the dam operation records indicated that the Eaton Wash stream gage record was impacted by outflows from the Eaton Wash dam by only three storms of the 27 year record (1969, 1980 and 1983 storms). The stream gage record was therefore modified according to the dam outflow hydrographs for these three storms. Hence, only the fully urbanized portion of Eaton Wash was used for the "model" calibration purposes.

Although all seven catchments are within a close vicinity of each other, they are located in two distinct groupings. Compton1, Compton2 and Dominguez are all neighboring catchments; whereas Arcadia, Alhambra, Eaton, and Rubio Washes are all located side-by-side with the same exposure to the incoming coastal storms. Because of the close similarities of the catchments in each of the two groupings, correlations between stream gage records are possible, which can then be used to supply any missing data points in the gage records or to check on the appropriateness of any adjustments made to the gage records due to dams, debris dams, or due to the effects of urbanization.

Peak Loss Rate, F_p

From Table 1, several peak rainfall loss rates are tabulated which include, when appropriate, two loss rates for double-peak storms. The range of values for all F_p estimates lie between 0.30 and 0.65 inch/hour with the highest value occurring in Verdugo Wash which has substantial open space in foothill areas. Except for Verdugo Wash, $0.20 \leq F_p \leq 0.60$ which is a variation in values of the order noted for Alhambra Wash alone. Figure 2 shows a histogram of F_p values for the several watersheds. It is evident from the figure that 88 percent of F_p values are between 0.20 and 0.45 inch/hour, with 77 percent of the values falling between 0.20 and 0.40 inch/hour. Consequently, a regional mean value of F_p equal to 0.30 inch/hour is proposed; this value contains nearly 80 percent of the F_p values, for all watersheds, for all storms, within 0.10 inch/hour.

S-Graph

Each of the watersheds listed in Table 1 has S-graphs developed for each of the storms where peak loss rate values were developed. For example, Fig. 3 shows the several S-graphs developed for Alhambra Wash.

By averaging the several S-graph ordinates (developed from rainfall-runoff data), an average S-graph was obtained. By combining the several watershed average S-graphs (Fig. 4) into a single plot, an average of averaged S-graphs is obtained. This regionalized S-graph (Urban S-graph in Fig. 4) can be proposed as a regionalized S-graph for the several watersheds. Indeed, the variation in S-graphs for a single watershed for different storms (see Fig. 3) is of the order of magnitude of variation seen between the several catchment averaged S-graphs. Such a regionalized S-graph can be developed for general regions classified as Valley, Foothill, Mountain, and Desert when the runoff data indicates similar tendencies. In this study, however, only the Valley region runoff data was considered.

In order to quantify the effects of variations in the S-graph due to variations in storms and in watersheds (i.e., for ungaged watersheds not included in the calibration data set), the scaling of Fig. 5 was used where the variable "X" signifies the average value of an arbitrary S-graph as a linear combination of the steepest and flattest S-graphs obtained. That is, all the S-graphs (all storms, all catchments) lie between the Feb. 1978 storm Alhambra S-graph ($X = 1$) and the San Jose S-graph ($X = 0$). To approximate a particular S-graph of the sample set,

$$S(X) = X\,S_1 + (1-X)\,S_2 \qquad (8)$$

where $S(X)$ is the S graph as a function of X, and S_1 and S_2 are the Alhambra (Feb. 1978 storm) and San Jose S graphs, respectively. Figure 6 shows the population distribution of X where each watershed is weighted equally in the total distribution (i.e., each watershed is represented by an equal number of X entries). Table 2 lists the X values obtained from the Fig. 5 scalings of each catchment S-graph. In the table, an "upper" and "lower" X-value that corresponds to the X coordinate at 80 percent and 20 percent of ultimate discharge values, respectively, is listed. An average of the upper and lower X values is used in the population distribution of Fig. 6.

TABLE 2. CATCHMENT S-GRAPH X-VALUES

WATERSHED NAME	STORM	X(UPPER)	X(LOWER)	X(AVG)
Alhambra	Feb. 78	1.00	1.00	1.00
	Feb. 80	0.95	.60	0.78
	Mar. 78	0.70	.80	0.75
Limekiln	Feb. 78	0.50	0.80	0.65
	Feb. 80	0.80	1.00	0.90(2)
Supulveda	AVG.	0.90	0.80	0.85(3)
Compton	AVG.	0.90	1.00	0.95(3)
Westminster	AVG.	0.60	0.60	0.60(3)
Santa Ana Delhi	AVG.	0.80	1.00	0.90(3)
Urban	AVG.	0.90	0.80	0.85

In the table, the numbers in parenthesis indicate a weighting of the average X value. That is, due to only the average S-graph (previously derived by the COE) being available, it is weighted to be equally represented in the sample set with respect to the other catchments. All the catchments listed in the table are considered to be "Valley" type watersheds that are fully developed with only minor (if any) effects due to foothill terrain.

Catchment Lag

In Table 2, the Urban S-graph, which represents a regionalized S-graph for urbanized watersheds in valley type topography, has an associated X value of 0.85. When the Urban S-graph is compared to the standard SCS S-graph, a striking similarity is seen (Fig. 7). Because the new Urban S-graph is a near duplicate of the SCS S-graph, it was assumed that catchment lag (COE definition) is related to the catchment time of concentration, Tc, as is typically assumed in the SCS approach.

Catchment Tc values are estimated by subdividing the watershed into subareas with the initial subarea less than 10 acres and a flow-length of less than 1000 feet. Using a Kirpich formula, an initial subarea Tc is estimated, and a Q is calculated. By subsequent routing downstream of the peak flowrate (Q) through the various conveyances (using normal depth flow velocities) and adding estimated successive subarea contributions, a catchment Tc is estimated as the sum of travel times analogous to a mixed velocity method.

Lag values are developed directly from available COE calibration data, or by using "basin factor" calibrated from neighboring catchments (see Fig. 1). The COE standard lag formula is:

$$\text{lag (hours)} = 24\ n \left(\frac{L\ L_{ca}}{s^{0.5}} \right)^{0.38} \tag{9}$$

where L is the watershed length in miles; L_{ca} is the length to the centroid along the watercourse in miles; s is the slope in ft/mile; and n is the basin factor.

Because Eaton Wash, Rubio Wash, Arcadia Wash and Alhambra Wash are all contiguous (see Fig. 1), have similar shape, slopes, development patterns, and drainage systems, the basin factor of $n = 0.015$ developed for Alhambra Wash was also used for the other three neighboring watersheds. Then the lag was estimated using Eq. 9.

Compton Creek has two gages, and the $n = 0.015$ developed for Compton2 was also used for the Compton1 gage. The Dominguez catchment, which is contiguous to Compton Creek, is also assumed to have a lag calculated from Eq. 9 using $n = 0.015$.

The Santa Ana-Delhi and Westminster catchment systems of Orange County have lag values developed from prior COE calibration studies. Figure 8 provides a summary of the local lag versus Tc data. A least-squares best fit results in

$$\text{lag} = 0.72\text{Tc} \tag{10}$$

McCuen et al. (1984) provide additional measured lag values and mixed velocity Tc estimates which, when lag is modified according to the COE definition, can be plotted with the local data such as shown in Fig. 9. A least-squares best fit results in:

$$\text{lag} = 0.80\text{Tc} \tag{11}$$

In comparison, McCuen (1982) gives standard SCS relationships between lag, Tc, and time-to-peak (Tp) which, when modified to the COE lag definition, results in:

$$\text{lag} = 0.77\text{Tc} \tag{12}$$

Adopting a lag of 0.80Tc as the estimator, the distribution of (lag/Tc) values with respect to Eq. 11 is shown in Fig. 10.

PARAMETER VERIFICATION

The three parameter distributions of loss rate F_p values, S-graph, and lag were used to simulate a severe storm of March 1, 1983, which was not included in the calibration set of storms. The March 1, 1983 storm was a multi-peaked storm event and the resulting model results for each of the Los Angeles watersheds are shown in Table 3.

The values for parameters used in the modeling results of Table 3 are F_p = 0.30 inch/hour; pervious cover = actual value; Urban S-graph; measured gage rainfall and storm pattern; and computed lag values from Eq. 11. Two sets of values for the low loss fraction, $\bar{Y}$, were used; namely (i) $\bar{Y}$ estimated from Eq. 3, and (ii) $\bar{Y}$ calibrated by taking $\bar{Y}$ equal to 1 - (measured storm runoff volume)/(measured storm rainfall). This second value of $\bar{Y}$ was calibrated (rather than using Eq. 3 due to the obvious variation in rainfall intensities over the watershed for the March 1 storm. Figure 11a provides a comparison between measured and modeled runoff hydrographs. Figure 11b shows the point rainfalls recorded at various gage locations. A comparison of Table 3 modeling results with other modeling results reported by

Loague and Freeze (1985), HEC Research Note No. 6 (1979), and the HEC Technical Paper No. 59 (Abbott, 1978) shows that the subject modeling verification results are promising.

TABLE 3. MARCH 1, 1983, PEAK FLOW ESTIMATES

			Regional Model			Calibrated to Low Loss Fraction, $\bar{Y}$		
Watershed	Time (Hours)	Recorded Q(CFS)	Std. Time	Modeled Q(CFS)	Relative Error	Std. Time	Modeled Q(CFS)	Relative Error
Arcadia[1]	0615	1460	0655	1830	+25	0655	1740	+19
	0845	3660	0900	3490	- 5	0900	3500	-4
	1215	4110	1215	1275	-69	1250	1260	-69
	2000	1340	1925	3550	+165	1925	3530	+163
Eaton[2,4]	0619	1780	0720	2005(+150)	+13	0715	2320(+150)	+30
	0904	4300	0925	5420(+150)	+26	0925	5510(+150)	+28
	1219	5430	1300	2570(+600)	-53	1300	2830(+600)	-48
	1934	3080	1950	5160(+750)	+68	1950	5310(+750)	+72
Rubio[3]	0630	1500	0700	2610	+74	0700	2450	+63
	0900	3760	0905	5980	+ 59	0905	5990	+59
	1215	2520	1245	2200	-13	1245	2110	-16
	1930	3520	1930	5920	+68	1930	5900	+68
Alhambra	0615	2290	0710	2405	+ 5	0710	2450	+7
	0830	7010	0915	6460	- 8	0915	6460	-8
	1200	5300	1255	1700	- 68	1255	2550	-52
	1900	5250	1940	5300	+ 1	1940	5320	+1
Compton2	0645	3380	0645	1290	- 62	0645	1237	-63
	0815	4620	0940	4160	-10	0940	4100	-11
	1200	2430	1200	2460	+ 1	1200	2320	-5
	1845	847	1955	970	+14	2010	920	+9
Dominguez	0910	9830	0925	6915	- 30	0925	7600	-23
	1206	6180	1240	4180	- 32	1240	5000	-19
	1900	2400	1955	1735	- 28	1955	2090	-13
	2400	1700	2440	1905	+12	2440	2370	+39

Notes: 1 - Area reduced 14% due to Debris Basins
2 - Area reduced 57% due to Eaton Dam
3 - Area reduced 3% due to Debris Basins
4 - ( ) added to modeled Q's to account for Eaton Wash Dam outflow (per LACFCD 1983 Storm Report)

PARAMETER UNCERTAINTY AND MODEL RESPONSE

The design storm/unit hydrograph model is to be used in Orange County for flood control study purposes. Due to the rapid urbanization of Orange County reflected in the local gage records, considerable uncertainty would result in modifying Orange County gage records for the effects of urbanization. In contrast, the Los Angeles gage records reflect nearly stable, fully developed conditions for over 30 years of record. Another important factor in the use of gage data is that the Orange County catchments typically have significant constrictions which severely impact the calibration of S-graphs and lag values but would be removed ultimately with further development.

In comparison, the Los Angeles gage records have nearly homogeneous gage records with free flowing, fully developed drainage systems. Additionally, the Los Angeles gages are within 10 miles of Orange County and are all subject to similar coastal influence. Consequently, the Orange County hydrology model is calibrated to the Los Angeles gage data, so that it can be transferred for use in Orange County watersheds. As a result, all parameter estimates from a standardized hydrology manual contain uncertainty. However, it is important to recognize that parameter estimates at a gage site are also uncertain, but the level of uncertainty would be much less than what occurs at an ungaged site.

Each of the "model" parameters (lag, F_p, and S-graph) for the Orange County watersheds are assumed to have the probability distribution functions (pdf) shown in a discrete histogram form in Figs. 2, 6, and 10 for F_p, S(X), and lag = 0.8Tc, respectively. For example, if the "model" is applied at a gaged site, say Alhambra Wash, then the variability in the S graph is not given by Fig. 6 for S(X), where $0.60 \le X \le 1$, but for $0.75 \le X \le 1$ (see Table 2). Similarly, the estimate for lag is much more certain for Alhambra Wash than shown in Fig. 10. Consequently, the uncertainty in the "model" output for a gaged site will show a significantly smaller range in possible outcomes than if the total range of parameter values of Figs. 6 and 10 are assumed (as is done for the ungaged sites, or sites where an inadequate length of data exist for a constant level of watershed development).

In Orange County, it is assumed that any of the parameter values can take the values shown in Figs. 2, 6, and 10 with the indicated frequencies. That is, a particular watershed may respond equally likely as Alhambra Wash or Compton1, or any of the catchments used in the calibration effort. Because the several catchment parameter values vary and overlap, the overall frequency of parameter value occurrences are assumed given by the distributions shown.

To evaluate the "model" uncertainty, a simlulation that exhausts all combinations of parameter values shown in the pdf distribution was prepared. Because the lag/Tc plot is a function of Tc, several Tc values were assumed and lag values varied freely according to Fig. 10. The re-resulting Q/Qm distribution is shown in Fig. 12 for the case of Tc equal to 1 hour and a watershed area of 1 square mile (hence, depth-area adjustments are not involved). In the figure, Q is a possible model peak flow rate outcome, and Qm is the peak flow rate obtained from the "model" assuming lag equal to 0.8 Tc, F_p equal to 0.30 inch/hour, and X equal to 0.85 (Urban S-graph). The Q/Qm plots were all very close to Fig. 12 as a function of Tc; therefore, Fig. 12 is taken to represent the overall Q/Qm distribution for watershed areas less than 1 mi^2.

The results of Fig. 12 show that a flood control hydrology manual which stipulates a procedure for estimating peak flow rates has an associated Q/Qm distribution that represents the variation in possible true values of Q (if the parameters were known exactly) from the design value Qm used for flood control design purposes. This modeling uncertainty must be coupled to flood frequency estimate uncertainty in order to achieve a specified level of confidence that Qm provides a given level of flood protection.

Not reflected in Fig. 12 is the additional uncertainty due to the choice of depth-area adjustments. One frequently used set (e.g., HEC TD#15, 1982) is the NOAA Atlas 2 data, which provide adjustments for 30-minute, 1-, 3-, 6-, and 24-hour durations. Another candidate set of curves are the COE-developed Sierra-Madre storm depth-area adjustments for use in southern California. The variation in adjustment factors is shown in Fig. 13. With only two data points for a pdf distribution, a statistical evaluation is impossible. However, it is assumed that the COE adjustment factors are more appropriate for the southern California region than the NOAA Atlas 2 curves, which are 'regionalized' for the entire United States. Consequently, depth-area effects are being considered "exactly known" in a probabilistic sense, which implies (incorrectly) that there is no significant uncertainty in the adjustment factors used.

The effects on model certainty due to the choice of either set of depth-area relationships is reflected in Figs. 14-16. The figures show the distribution of Q/Qm for watershed areas of 5, 50, and 100 mi^2, respectively, and for an intermediate design storm frequency of 25 years. In Fig. 15 it is seen that the COE depth-area curves result in such a significant adjustment of point rainfall values in the design storm that the Q/Qm range of outcomes is considerably less than when using the NOAA Atlas 2 set. That is, the error distribution of the "model" Q/Qm has a smaller range of values when using the COE depth-area curves than when using the NOAA Atlas 2 curves.

An important question arises as to whether or not the distribution of outcomes from the calibrated model can be reduced (i.e., the model made more certain) by introducing additional parameters. It is not clear in the current literature whether such a claim has validity. However, some pointed remarks can be taken from Klemes and Bulu (1979) who evaluate the "limited confidence in confidence limits derived by operational stochastic hydrologic models." They note that advocates of modeling "sidestep the real problem of modeling--the problem of how well a model is likely to reflect the future events--and divert the user to a more tractable, though less useful, problem of how best to construct a model that will reproduce the past events." In this fashion, "by the time the prospective modeler has dug himself out of the heaps of technicalities, he either will have forgotten what the true purpose of modeling is or will have invested so much effort into the modeling game that he would prefer to avoid questions about its relevance." Of special interest is their conclusion that "Confidence bands derived by more sophisticated models are likely to be wider than those derived by simple models." That is, "the quality of the model increases with its simplicity."

In a reply by Nash and Sutcliffe (1971) to comments by Fleming (1971), the simple model structure used by Nash and Sutcliffe (1971) is defended as to modeling completeness in comparison to the Stanford Watershed Model variant, HSP. Nash and Sutcliffe write that "...We believe that a simple model structure is not only desirable in itself but is essential if the parameter values of the component parts are to be determined reliably through an optimization procedure.... One must remember that the data always constitute a limited sample and the optimized values are 'statistics' derived from this sample and therefore subject to sampling variance. The more complex the model structure the greater is the difficulty in obtaining optimum parameter values with low sampling variance. This difficulty becomes particularly acute...when two or more model components are similar in their operation..."

Should a comparison be made between a simple model, such as described herein, and an 'advanced model', the results would not be conclusive. As Nash and Sutcliffe write that "...The more complex model would almost certainly provide a better fit, as a linear regression analysis on a large number of variables will almost invariably provide a better fit than one of those independent variables whose significance has been established." Hence, the hydrologist must be careful to evaluate modeling results obtained from a verification test rather than obtained from a calibration data set. Nash and Sutcliffe also note the dominating importance of errors in rainfall and effective rainfall estimates in complex models such as HSP: "We wonder, however, how the parameters expressing spatial variation of rainfall or infiltration capacity, can be optimized at all, let alone with stability or significance, in the typical case where the short-term rainfall data are based on a single recording rain gauge, as in Dr. Fleming's first example."

REFERENCE LIST

1. Beard L., Chang S., Journal of the Hydraulics Division, Urbanization Impact on Streamflow, June, 1974.

2. Chow V., Kulandaiswamy V., The IUH of General Hydrologic Systems Model, Journal of the Hydraulics Division, Proceedings of the American Society of Civil Engineers, Vol. 108, No. HY7, July, 1982.

3. Fleming G., Franz D., Flood Frequency Estimating Techniques for Small Watersheds, Journal of the Hydraulics Division, Vol. 97, No. HY9, September, 1971.

4. Klemes V., Bulu A., Limited Confidence in Confidence Limits Derived by Operational Stochastic Hydrologic Models, Journal of Hydrology, 42(1979) 9-22, Elsevier Scientific Publishing Company, Amsterdam, printed in the Netherlands.

5. Loague K., Freeze R., A Comparison of Rainfall-Runoff Modeling Techniques on Small Upland Catchments, Water Resources Research, Vol. 21, No. 2, February, 1984.

6. McCuen R., Bondelid T., Estimating Unit Hydrograph Peak Rate Factors, Journal of Irragation and Drainage Engineering, Vol. 109, No. 2, June, 1983.

7. McCuen R., et al, Estimating Urban Time of Concentration, Journal of Hydraulic Engineering, Vol. 110, No. 7, July, 1984.

8. McCuen R., et al, SCS Urban Peak Flow Methods, Journal of Hydraulic Engineering, Vol. 110, No. 3, March, 1984.

9. Nash J., Sutcliffe J., River Flow Forecasting Through Conceptual Models Part 1 - A Discussion of Principles, Journal of Hydrology, 10 (1970) 282-290.

10. Schilling W., Fuchs L., Errors in Stormwater Modeling - A Quantitive Assessment, Journal of Hydraulic Engineering, Vol. 112, No. 2, February, 1986.

11. Scully D., Bender D., Separation of Rainfall Excess from Total Rainfall, Water Resources Research, Vol. 5, No. 4, August, 1969.

12. U.S. Army Corps of Engineers, The Hydrologic Engineering Center, Adoption of Flood Flow Frequency Estimates at Ungaged Locations, Training Document No. 11, February, 1980.

13. U.S. Army Corps of Engineers, The Hydrologic Engineering Center, Comparative Analysis of Flood Routing Methods, Resaerch Document No. 24, September, 1980.

14. U.S. Army Corps of Engineers, The Hydrologic Engineering Center, Continuous Hydrologic Simulation of the West Branch Dupage River above West Chicago: An Application of Hydrocomp's HSP, Research Note No. 6.

15. U.S. Army Corps of Engineers, The Hydrologic Engineering Center, Hydrologic Analysis of Ungaged Watersheds Using HEC-1, Training Document No. 15, April, 1982.

16. U.S. Department of Transportation, Federal Highway Administration, Hydrology, Hydraulic Engineering Circular No. 19, October, 1984.

17. U.S. Army Corps of Engineers, The Hydrologic Engineering Center, Introduction and Application of Kinematic Wave Routing Techniques Using HEC-1, Training Document No. 10, May, 1979.

18. U.S. Army Corps of Engineers, The Hydrologic Engineering Center, Testing of Several Runoff Models on an Urban Watershed, Technical Paper No. 59.

19. U.S. Department of Agriculture, Soil Conservation Service, National Engineering Handbook Section 4 (NEH-4) 210-V1 Amendment 5, Transmission Losses, Washington, D.C., March 1, 1983.

20. Williams D.W. et al, TRRL and Unit Hydrograph Simulations Compared with Measurements in an Urban Catchment, Journal of Hydrology, 48(1980) 63-70, Elsevier Scientific Publishing Company, Amsterdam - printed in the Netherlands.

Fig. 1. Location of Drainage Basins.

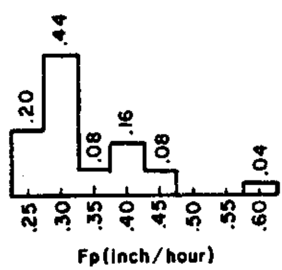

Fig. 2. HISTOGRAM OF SOIL LOSS FUNCTION

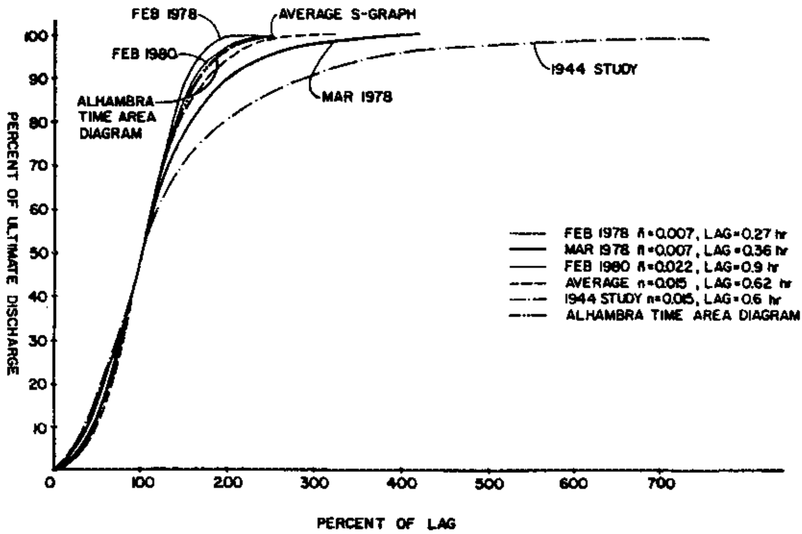

Fig. 3 Alhambra Wash S-Graphs

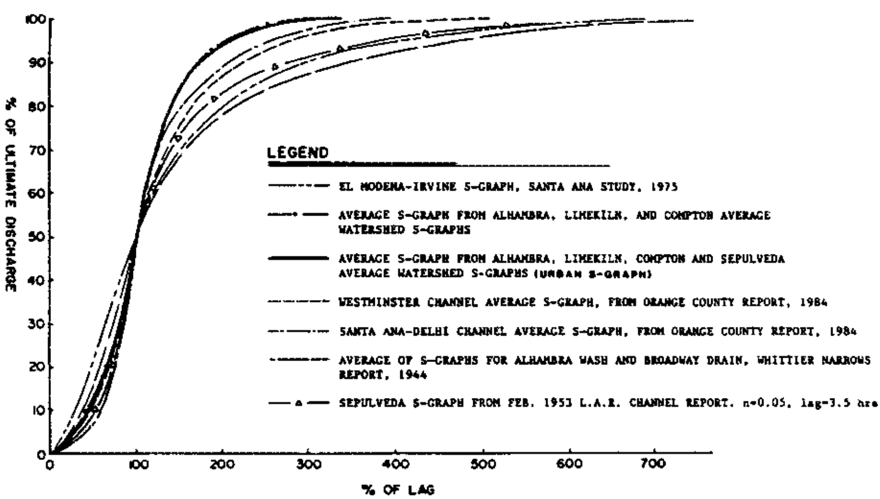

Fig. 4 Average S-Graphs

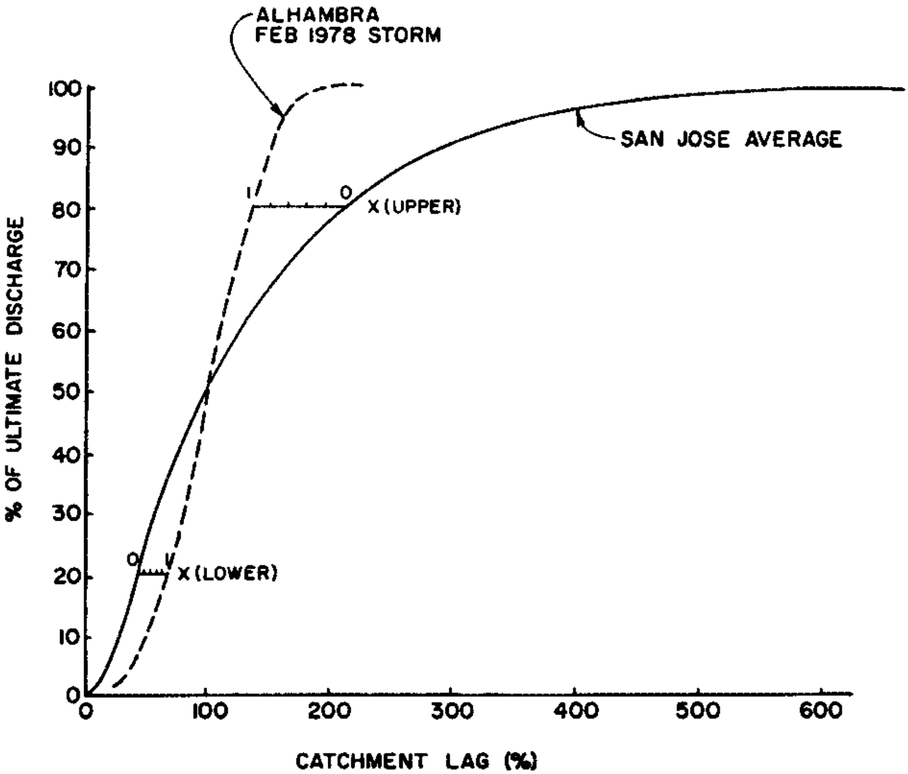

Fig. 5. S-Graph Scaling for S(X).

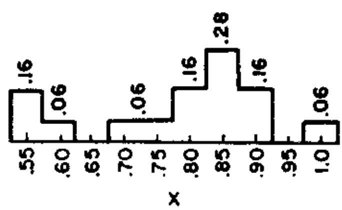

Fig. 6. HISTOGRAM OF VARIATION IN S-GRAPH

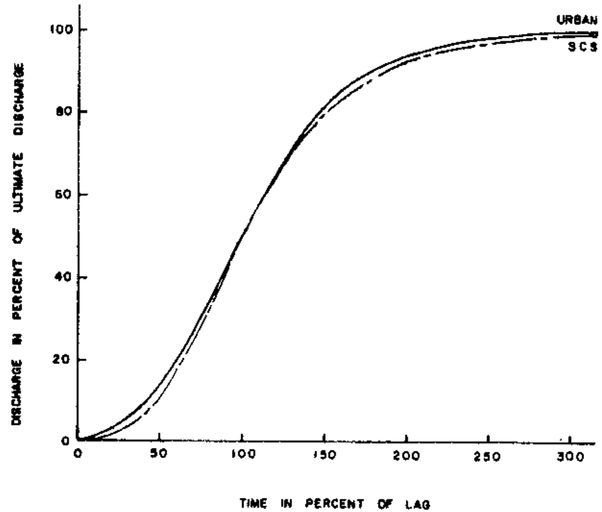

Fig. 7. Comparison of SCS and Urban S-Graphs.

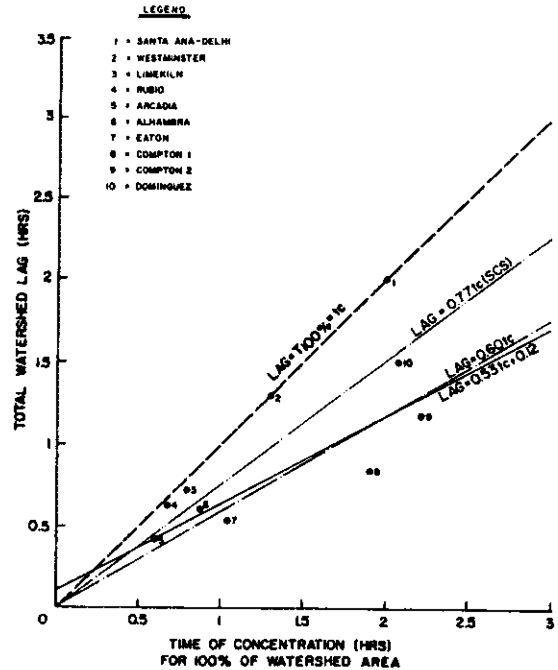

Fig. 8. Relationship Between Catchment Lag and Tc Values for Local Region.

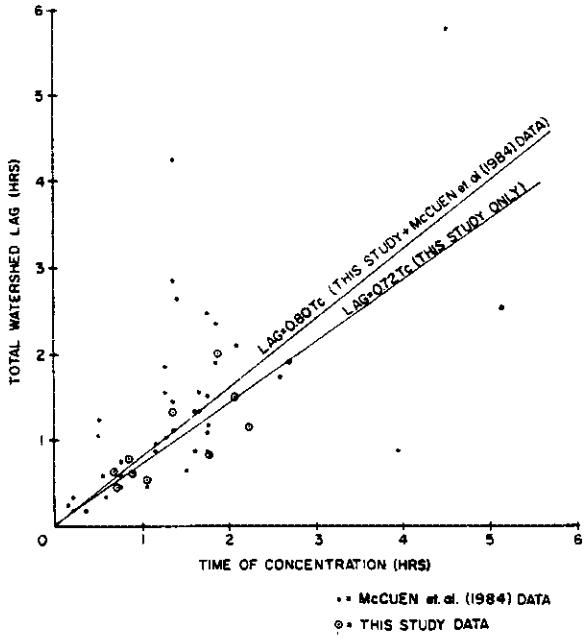

Fig. 9. Relationship Between Measured Catchment Lag and Computed Tc.

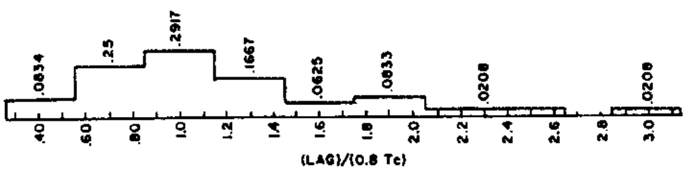

Fig. 10. HISTOGRAM OF LAG TIME

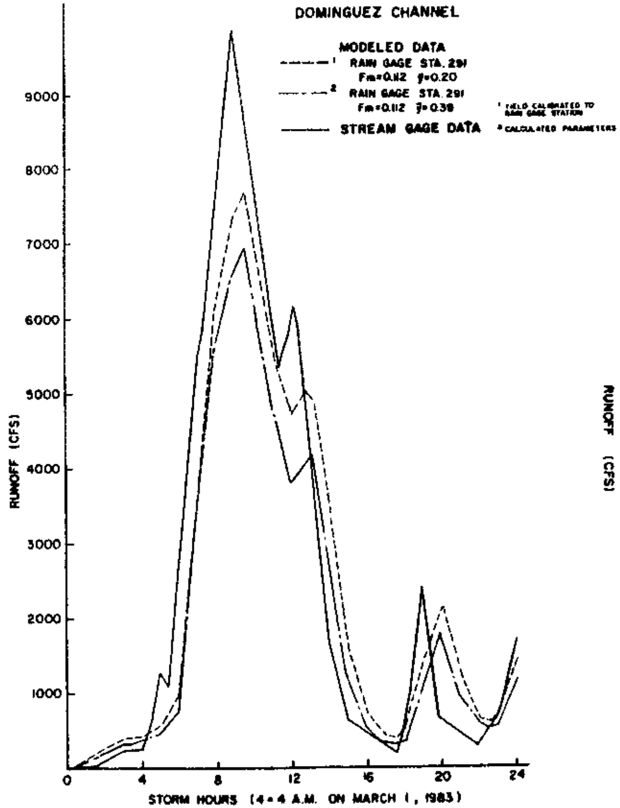

Fig. 11a. March 1, 1983 Runoff Hydrographs (2 of 6).

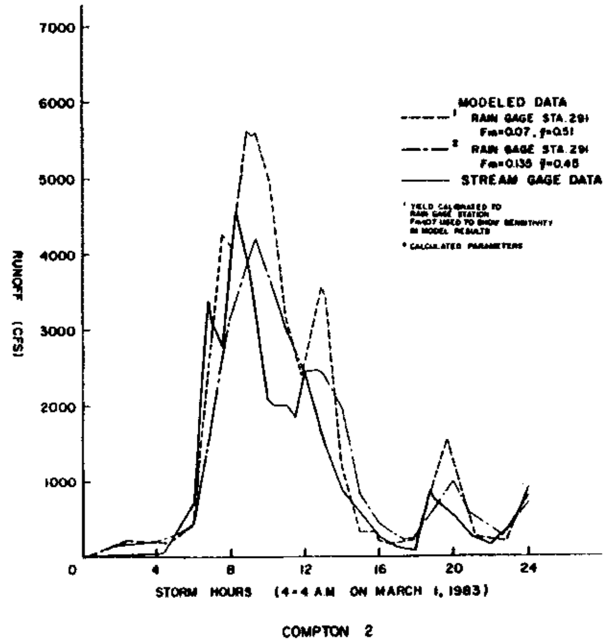

Fig. 11a. March 1, 1983 Runoff Hydrographs (1 of 6).

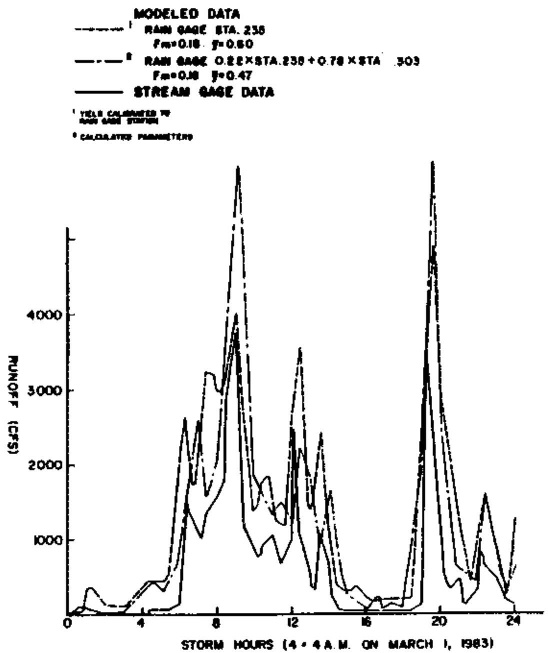

RUBIO WASH

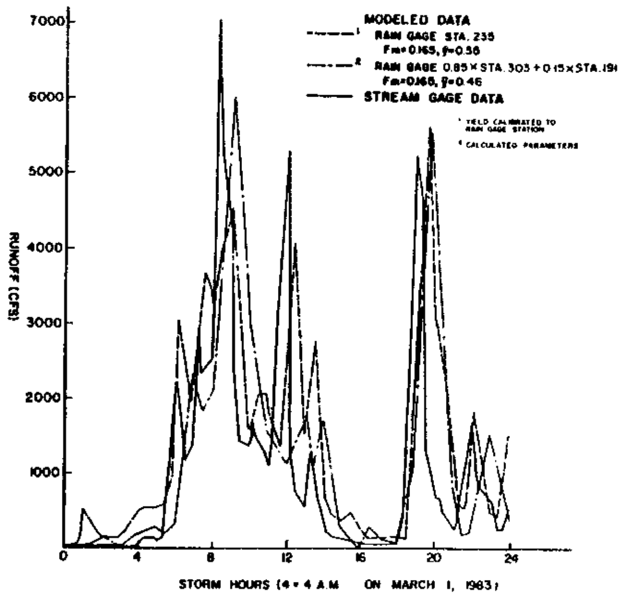

ALHAMBRA WASH

Fig. 11a. March 1, 1983 Runoff Hydrographs (3 of 6). Fig. 11a. March 1, 1983 Runoff Hydrographs (4 of 6).

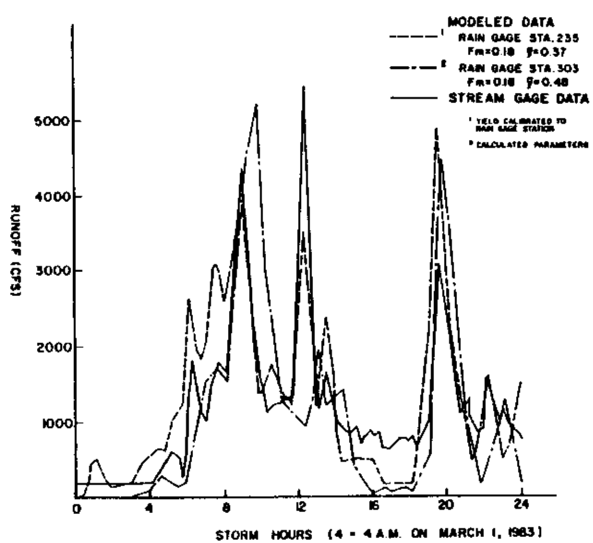

EATON WASH

Fig. 11a. March 1, 1983 Runoff Hydrographs (5 of 6).

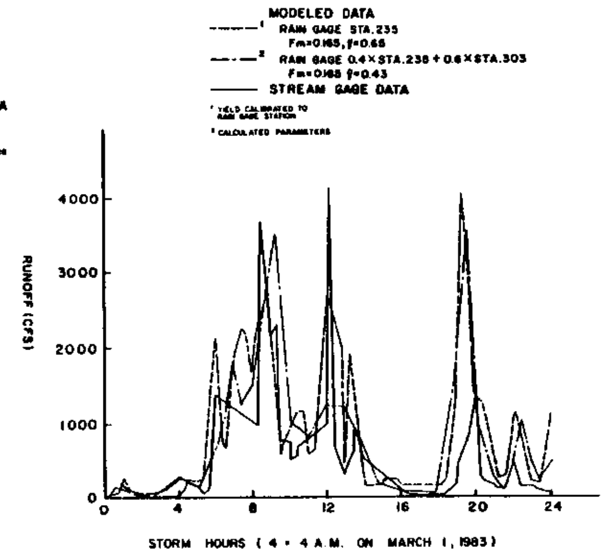

ARCADIA WASH

Fig. 11a. March 1, 1983 Runoff Hydrographs (6 of 6).

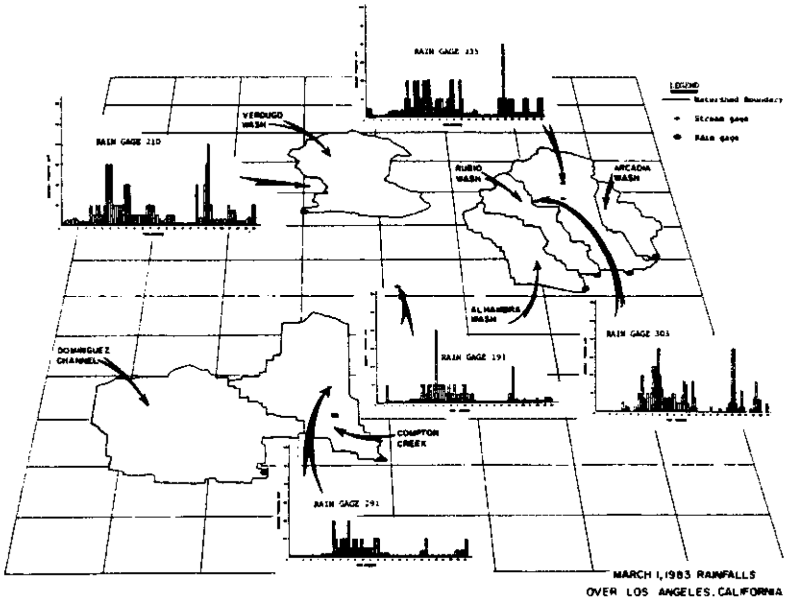

Fig. 11b. March 1, 1983 Storm Rainfall Patterns.

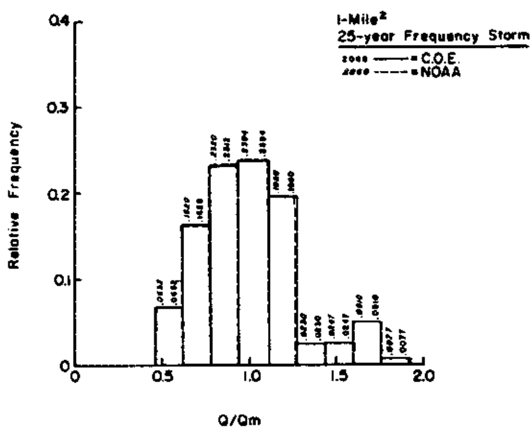

Fig. 12. Q/Qm Distribution for Tc= 1-hour, Area= 1-mi.^{2}, and COE or NOAA Depth-Area Adjustments.

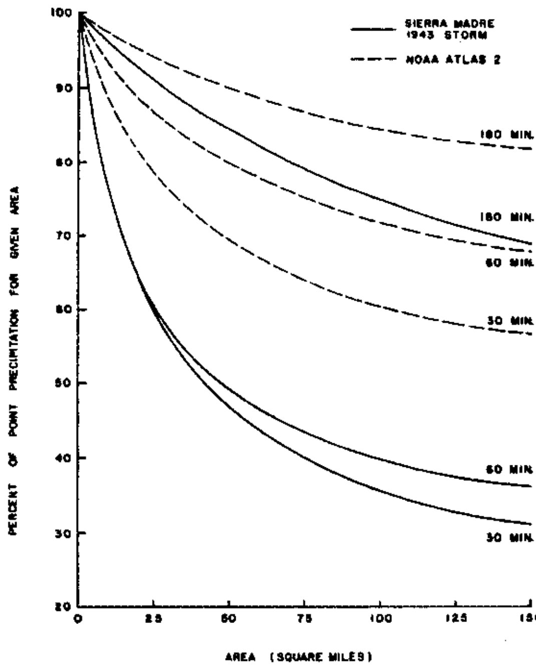

Fig. 13. Depth-Area Adjustment Curves.

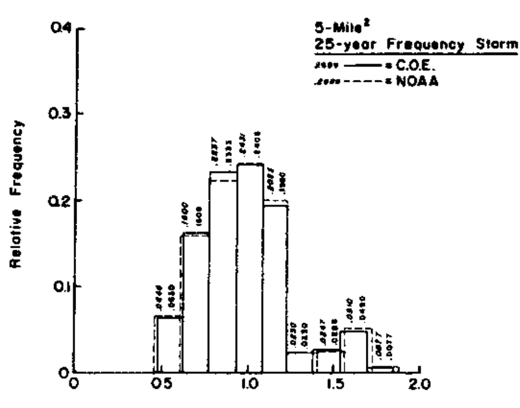

Fig. 14. Q/Qm Distribution for 5-mi.^{2} Area.

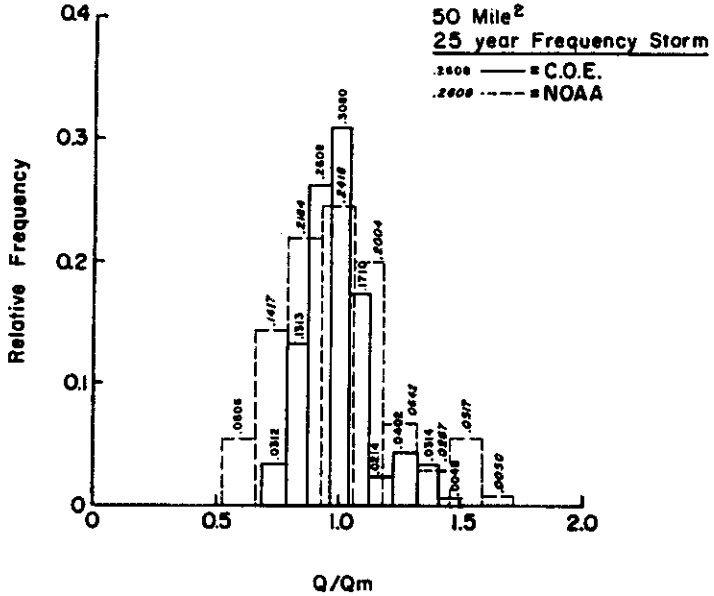

Fig. 15. Q/Qm Distribution for 50-mi.^{2} Area.

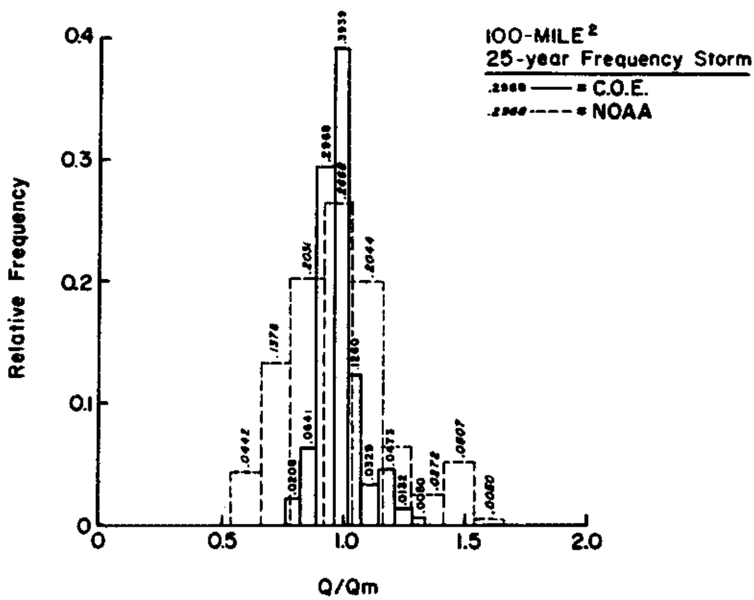

Fig. 16. Q/Qm Distribution for 100-mi.^{2} Area.